A new interpretation of the sedimentary cover in the western Siljan Ring area, central Sweden, based on seismic data

Christopher Juhlin [a,*], Erik Sturkell [b], Jan Ove R. Ebbestad [c], Oliver Lehnert [d], Anette E.S. Högström [e], Guido Meinhold [f]

[a] Department of Earth Sciences–Geophysics, Uppsala University, Villavägen 16, SE-752 36 Uppsala, Sweden
[b] Department of Earth Sciences, University of Gothenburg, PO Box 460, SE-405 30 Göteborg, Sweden
[c] Museum of Evolution, Uppsala University, Norbyvägen 16, SE-752 36 Uppsala, Sweden
[d] GeoZentrum Nordbayern, Universität Erlangen, Schloßgarten 5, D-91054 Erlangen, Germany
[e] Tromsø University Museum, Natural Sciences, N-9037 Tromsø, Norway
[f] Sedimentology and Environmental Geology, Geoscience Centre, University of Göttingen, Goldschmidtstrasse 3, D-37077 Göttingen, Germany

ARTICLE INFO

ABSTRACT

Two new reflection seismic profiles over the Paleozoic successions of the western part of the Siljan Ring impact structure show a contrasting seismic signature. The more southerly c. 10 km long Mora profile reveals a highly disturbed structure, with only a few kilometers of relatively horizontally layered structures observed. However, interpretations of refracted arrivals in the data, that can be correlated to reflections, indicate the Silurian clastic rocks to be about 200 m thick in the central part of the profile. Weak reflections from about 600 m depth suggest a 400 m thick Ordovician limestone sequence to be present. Cores from the area show a mainly shale lithology for the Silurian and only a thin sequence of Ordovician strata, suggesting a rapid thickening of the Ordovician towards the north. On the more northern c. 12 km Orsa profile clear reflections from the Paleozoic successions are seen along the entire profile, except on the southernmost few kilometers. Based on interpretations of refracted arrivals, the Silurian succession appears to be considerably thinner here, and possibly absent at some locations. The Ordovician is also interpreted to be thinner in this area, with a maximum thickness of about 200–300 m along most of the profile. A deeper reflection from about 2 km within the crystalline basement may represent a dolerite sill. The lack of clear basement reflections on the Mora profile can be attributed to near-surface conditions and the acquisition geometry. The seismic data and recent coring in the area suggest the presence of a deeper paleo-basin towards the southwest with significantly more shales being deposited and the Paleozoic successions being severely disturbed. The shallow coring and seismic data will help form the basis for locating future boreholes for deeper drilling to study impact processes and the Paleozoic evolution of central Sweden.

© 2012 Elsevier B.V. Open access under CC BY-NC-ND license.

1. Introduction

During the summer of 2011 two reflection seismic profiles were acquired in the western part of the Siljan impact structure (Fig. 1). The work was conducted under the framework of the project 'Concentric Impact Structures in the Paleozoic' (CISP), which aims to study impact mechanics, tectonics and the paleobiology of the Siljan and Lockne impact structures. CISP is financed 2010–2012 by the Swedish Research Council (VR) as one of two currently VR funded projects that are part of the Swedish Deep Drilling Program (SDDP; Lorenz, 2010). To date, the overall objective for the CISP studies has been to establish reliable geological models for the planned deeper drilling in the Siljan and Lockne

impact structures under the SDDP umbrella; for an outline of detailed scientific objectives see Högström et al. (2010).

Acquisition of new reflection seismic data has been the first step in defining the drilling locations in the Siljan impact crater. Previously acquired seismic data in the area were obtained in conjunction with the search for abiogenic methane in the 1980s and early 1990s (Bodén and Erikson, 1988). A total of nine lines were acquired, mostly in the eastern and northern parts of the Siljan Ring area, but one of them, Line 9, extended from the central part of the crater nearly to the town of Mora (Fig. 1). These profiles show the upper crustal Transcandinavian Igneous Belt (TIB) granitic rock in the area to be fairly transparent, but with strong high amplitude sub-horizontal reflections at distinct levels in the upper 10 km. Deep drilling within the crater rim revealed these high amplitude reflections to be generated by relatively thin (5–50 m) dolerite sills (Juhlin, 1990; Papasikas and Juhlin, 1997). A deeper reflective zone is present at about 12–15 km throughout the area (Juhojuntti

* Corresponding author. Tel.: +46 18 4712392; fax: +46 18 501 110.
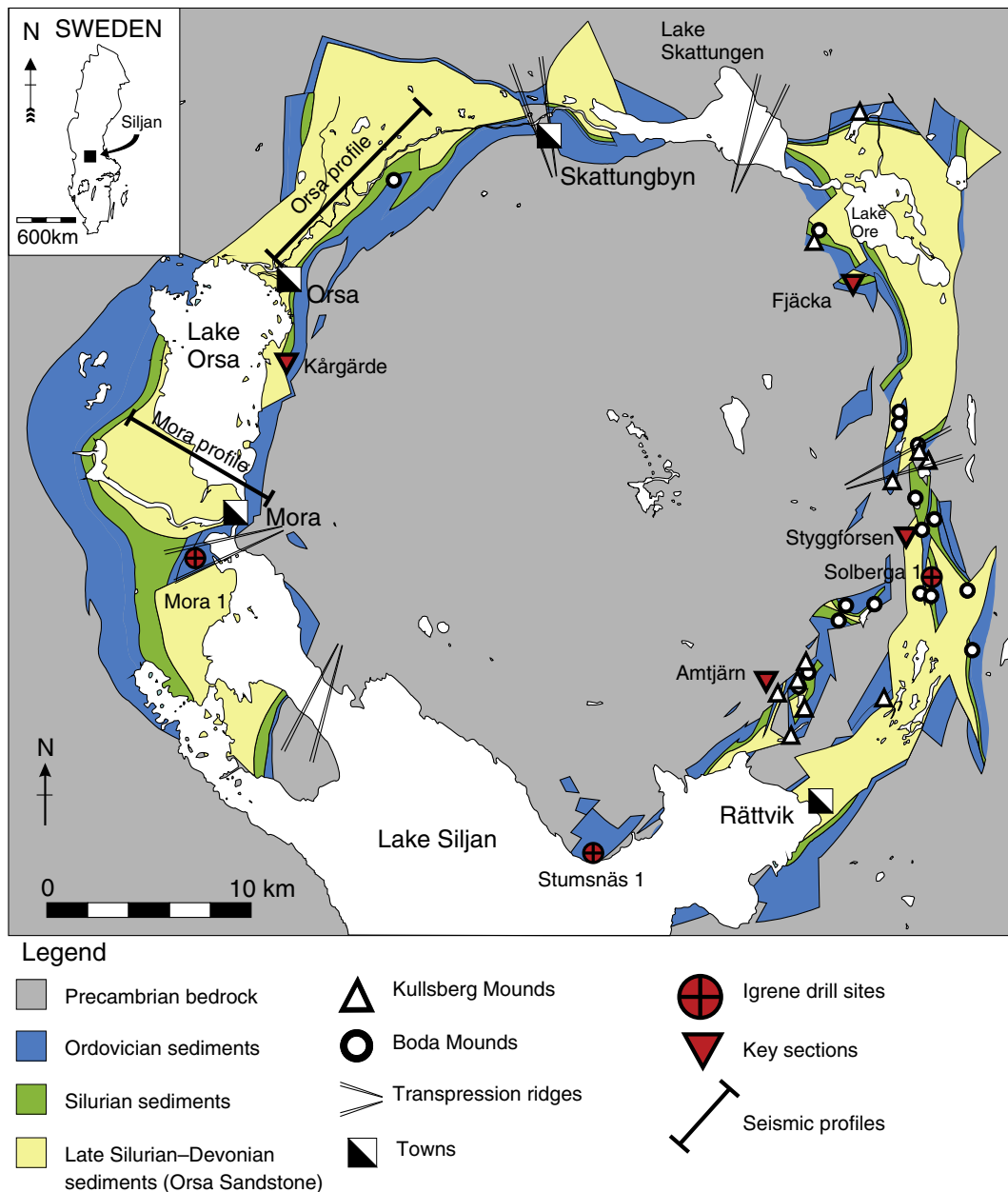E-mail address: Christopher.Juhlin@geo.uu.se (C. Juhlin).

Fig. 1. Location map of the Siljan Ring, showing distribution of sedimentary rocks, key geological sections, the drill sites for cores taken by Igrene AB, the position of the new seismic profiles, and the transpression ridges of Kenkmann and von Dalwigk (2000a,b).
Modified from Ebbestad and Högström (2007).

and Juhlin, 1998) that may have a different origin. North of the Siljan Ring, where Svecofennian Domain rocks are present at the surface, relatively strong lower crustal reflectivity is observed with the Moho interpreted to be at about 45 km (Juhojuntti and Juhlin, 1998).

In this paper we present results from two new seismic profiles that mainly pass over the Paleozoic sedimentary successions of the western part of the Siljan Ring. One profile, about 10 km long and striking in the W–E direction, was located just north of the town of Mora and extends onto the crystalline basement at its eastern end (Fig. 1). The other, about 12 km long and striking SW–NE, was located north of the town of Orsa and traversed only Paleozoic rocks (Fig. 1). Objectives of the profiles were to map the thickness of the sedimentary rocks and their internal structure, and if possible, identify structures in the crystalline basement below. Results from the profiles will be used as a starting point for defining future deep drilling locations in the area.

2. Geological setting

The Siljan structure was formed by a bolide that impacted the terrestrial landscape of central Sweden in the late Devonian (latest Frasnian; 377 Ma, Reimold et al., 2004, 2005). The structure is concentric with a central rise composed of Proterozoic magmatic rocks or younger Proterozoic meta-sediments and meta-volcanic rocks (western side) across a 33 km wide area in the east–west direction. The obvious circular structure outside the central rise (here called the ring) is outlined mainly by a ring of lakes and consists largely of marine Ordovician and Silurian sediments and Silurian to Devonian terrestrial sandstones, extending the east–west diameter to about 45 km (Fig. 1). It is northern Europe's largest crater, and may have played a casual role in the Fransnian/Famennian mass extinction (Reimold et al., 2004).

The transient crater that formed at impact may have been anywhere between 22 and 42 km (Grieve, 1988; Holm et al., 2011; Juhlin and Pedersen, 1987, 1993; Kenkmann and von Dalwigk, 2000a). The preserved central rise may represent the peak ring (Grieve, 1988), although Henkel and Aaro (2005) suggested that the peak ring was 20 km wide. The final diameter of the crater may have been anywhere between 52 and 90 km (Grieve, 1988; Henkel and Aaro, 2005; Holm et al., 2011; Kenkmann and von Dalwigk, 2000a,b) (Fig. 2).

The ring structure itself has been denoted as an annular ring graben, a mega-block zone, or a mega-breccia (Collini, 1988; Henkel and Aaro, 2005; Juhlin and Pedersen, 1987). Within the mega-blocks the Paleozoic successions are partly well preserved, albeit poorly exposed, and the stratigraphy is often continuous. It is clear that the mega-blocks now preserved in the ring could not have been within the transient crater, but rather represent radial inflow of the collapsed rim of the transient crater in concert with mass flow from the central area (Henkel and Aaro, 2005). A large transient crater would imply significant horizontal displacements of the mega-blocks (6–7 km; Kenkmann and von Dalwigk, 2000b), while a smaller crater would imply primarily vertical movements of blocks through localized sagging (listric faulting), which is what the reflection seismic data show in this paper, as well as in Juhlin and Pedersen (1987, 1993).

Even though the reflection seismic data indicate a relatively simple structure, at the scale of the resolution of the data, there are geological indications of more complex structures in the area. Outcrops in the Siljan Ring are few, but the heavily tectonized nature of the sedimentary successions is often evident, generally with sharply inclined or nearly overturned packages of crystalline basement and/or sediments. One of the more important sedimentary features in the area is the large Late Ordovician Boda Limestone mud mounds, which are quarried commercially. Several of these are steeply inclined and all are heavily fractured (mega-brecciated; Henkel and Aaro, 2005) as a result of immediate post-impact disturbances.

Recent investigations of new drill cores from the Siljan Ring have dramatically changed the established stratigraphic view of the successions within the ring (Lehnert et al., 2012). Instead of the classical Ordovician carbonate succession separated by a stratigraphic gap from the Silurian shale dominated sequence, it is now clear that several facies belts exist. During the Middle–Late Ordovician there was a carbonate platform succession towards the present day east, separated by a backbulge basin from the peripheral to the present day west in the Mora area. In Mora an erosional unconformity is observed, showing a considerable hiatus spanning the early Darriwilian to the upper Llandovery (preliminary dating; Lehnert et al., 2012). About 224 m of Silurian strata overlay
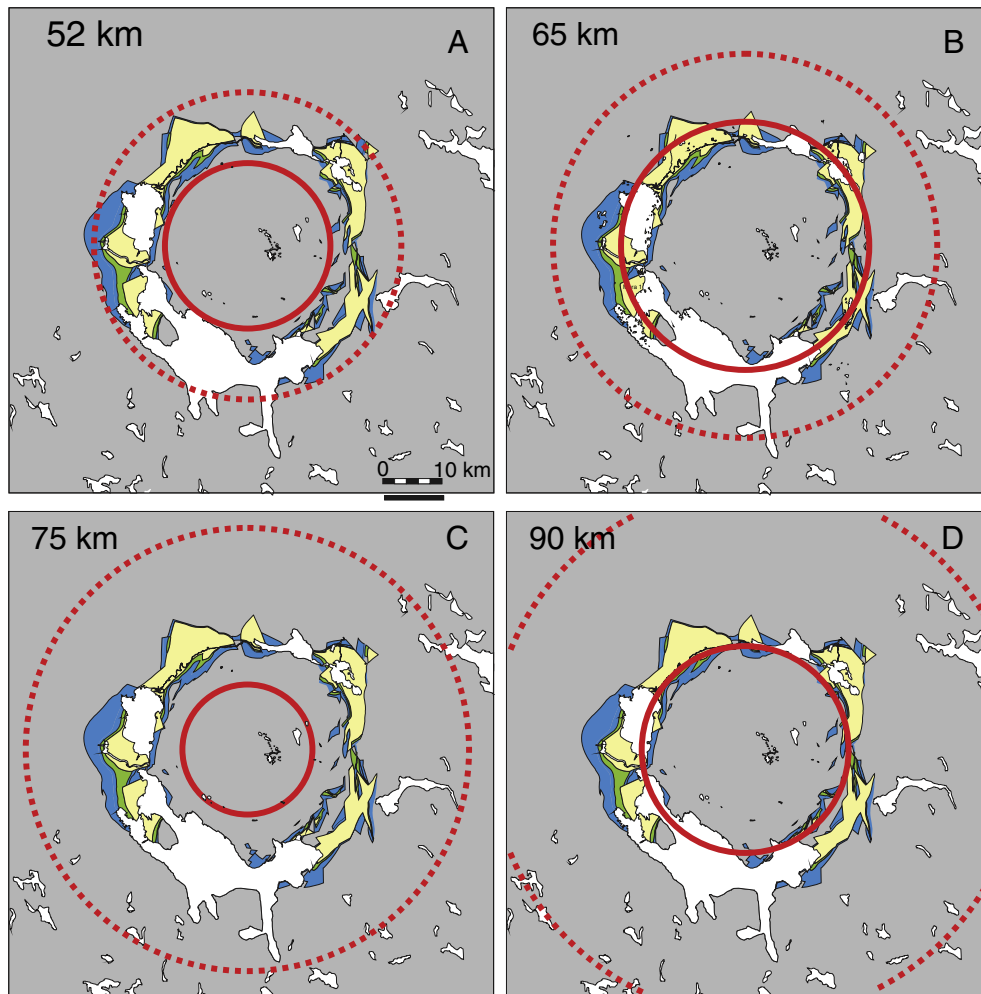

Fig. 2. Crater models developed for the Siljan impact structure. The entire circles denote the diameter of the transient crater, while the stippled circle denotes the diameter of the final crater. The center of the crater is based on estimates by Juhlin and Pedersen (1987). (a) A final crater measuring 52 km and pre-erosion transient crater measuring 26 km. Estimates by Grieve (1988) and Juhlin and Pedersen (1993) based on seismic studies. (b) A 42 km transient crater and a final size of 65 km. Based on Kenkmann and von Dalwigk (2000a) who delimited the size from distribution of fractures in the crystalline bedrock interpreted as impact-related. (c) A final crater of at least 75 km, with the inner ring he showing the estimated peak ring. Based on geomorphological data by Henkel and Aaro (2005). (d) A transient crater with a pre-erosion mean diameter of 35 km and a final size of 90 km. Based on the 32–38 km estimate of the transient crater and the maximum final diameter suggested by Holm et al. (2011), from distribution of shock metamorphic features.

here a thin Lower–Middle Ordovician carbonate succession (about 21 m) in the Mora 001 core (Fig. 1), drilled and owned by Igrene AB. There is no evident contact to the Orsa Sandstone or equivalent strata as is consistent with the partly coeval Nederberga Formation in the Skattungbyn area in the northern part of the ring structure (Fig. 1). The age of the uppermost preserved strata exposed at Mora is yet to be determined.

Earlier acquired reflection seismic data show approximately 350 m of Paleozoic sediments preserved above the crystalline basement in the eastern part of the ring (Collini, 1988), and Thorslund (in Rondot, 1975) estimated a total of 400–500 m of these sediments to be present. Where exposed, the sedimentary successions start with the Tremadocian, although Cambrian sediments may also be present in the area (Ebbestad and Högström, 2007). There are no continuous sections in the Siljan area, so the stratigraphy has been pieced together from a few key sections such as Kårgärde near the town of Orsa, Fjäcka on the northeast side of the ring, Amtjärn near the town of Rättvik, Styggforsen near Boda Church and the new Igrene drill cores (see Fig. 1). Exposures of the Ordovician–Silurian boundary are seen in a few quarries where the large Boda Limestone mud mounds are exposed. The development of strata in between the larger mounds and the Silurian succession has not been well understood, and the transition to the terrestrial Silurian/Devonian Orsa Sandstone is only seen in a few drill cores (Petalas, 1985). As a consequence, the total thickness of the Paleozoic succession in the Siljan Ring is not known and, with respect to distinct facies belts, may have been variable depending on the different paleo-environments. Regardless, the Siljan area has become the standard reference area for a number of Ordovician and Silurian type formations, units and/or biozones in Sweden (see Bergström, 2007).

Rough calculations of sediment thickness using measurements quoted for each unit in Ebbestad and Högström (2007) and Lehnert et al. (in press) suggest that the classic Ordovician succession is at the minimum 115 m thick and more than 133 m thick, albeit here excluding the ~35 m thick Kullsberg mounds and the ~100 m thick Boda mounds which formed during Late Ordovician times on the outer platform. Adding the thickness of the Boda Limestone (e.g. thickness of all beds from the *Obolus* beds to the Fjäcka Shale plus Boda Limestone), gives an estimate of between 185 and 215 m for the Ordovician sediments. In the Mora 001 core, the Silurian succession is at least 224 m thick (Lehnert et al., 2012), although it does not reflect the depositional thickness over the entire Siljan area. The thickest succession of Orsa Sandstone known is at least 58.9 m (Petalas, 1985). Adding up these highly uncertain estimates gives a minimum thickness of the Paleozoic sediments in the order of 460 to 500 m.

3. Data acquisition

Seismic data (Table 1) were acquired along two profiles in the western part of the Siljan Ring area in the summer of 2011 (Fig. 1). Since objectives were to both image the Paleozoic sedimentary rocks and the deeper crystalline basement (down to 3 km) along longer profiles a compromise between station spacing and profile length was necessary. In addition, it was expected that signal penetration could be an issue at some locations due to large amounts of sand in the near-surface. Therefore, a relatively powerful source with a source spacing of 20 m and a receiver spacing of 10 m was employed. If the Paleozoic rocks extend down to 500 m then this source and receiver spacing corresponds to an effective fold of about 25 at this depth with a normal moveout (NMO) stretch of about 50%. At 250 m depth the effective fold is half of this. This lower fold at shallower depth implies that degraded images in those parts of the final stacked section where the source coupling was poor may be expected.

Data were first acquired along the Mora profile during a 6 day period in the beginning of June 2011 using a tractor mounted mechanical hammer (see Juhlin et al. 2010 for details on the source). Acquisition started on the eastern end of the profile on granitic bedrock and proceeded westwards. It was not possible to lay cables across the outlet to Lake

Table 1
Data acquisition.

	Mora	Orsa
Spread type	Split	
Number of channels	320 (160–160)	
Near offset	0 m	
Geophone spacing	10 m	
Geophone type	28 Hz single	
Source spacing	20 m	
Source type	VIBSIST 3000	
Hit interval between hammer blows	100–200 ms	
Sweeps per source point	3–4	
Nominal fold	80	
Recording instrument	SERCEL 428UL	
Sample rate	1 ms	
Field low cut	Out	
Field high cut	400 Hz	
Record length	30 s	
Profile length	10 km	12 km
Source points	391	542
Dates acquired	3/6–9/6, 2011	10/6–15/6, 2011

Orsa (stations 1016–1035 in Fig. 3) so the acquisition geometry had to be adjusted in this area. A cabled fixed spread was used east of the outlet with 36 wireless units west of the outlet while the source was active on the eastern part. When all possible source points had been activated east of the outlet the cabled spread was moved to the west of the outlet and the 36 wireless units to the east of it. This strategy allowed us to acquire data to fill the gap below the outlet without having to repeat source points and avoided us having to transport the source back and forth through the town of Mora. In addition to the logistics with the outlet, there were many locations along the Mora profile where the source could not be activated due to the near-surface being too soft or that the profile ran too close to residential areas. These locations were mostly on the eastern half of the profile (Fig. 3). Surface deposits east of the Lake Orsa outlet consist mainly of moraine while west of the outlet the surface deposits are mainly glacial and fluvial sands.

After completing the Mora profile the spread was moved to the Orsa profile (Fig. 4) and acquisition continued using the same mechanical source. Logistics were less problematic along the Orsa profile, but there were some locations in the southern part of the profile where it was not possible to activate the source (Fig. 4). South of station 350 surface deposits are mainly fluvial sands while to the north of it glacial deposits dominate. In addition to the cabled spread that was rolled along during the acquisition, twelve 3-component wireless units were placed out along the profile at a spacing of 1 km. These units recorded nearly all of the source points during the acquisition, but presentation of data from these units is not the focus of this paper. However, these data may be useful in the future for building velocity models based on refracted waves.

4. Data processing

Data were decoded using a shift and stack method based on Park et al. (1996). Data quality varied significantly along the profiles depending upon the near surface conditions. The thickness of the uppermost loose deposits varies considerably in the area, as does the groundwater level. Interestingly, the depth to the groundwater level appeared to have less influence on the data quality than may have been expected. First break quality is nearly the same regardless of how much dry sand is present (Fig. 5). The thickness of the groundwater bearing loose sediments appears to be a more important factor influencing data quality. Where these loose sediments are thick a very 'ringy' signal after the first arrival is present. This signal masks weaker reflections and multiple reflections are generated that arrive within a cone that is limited by a velocity of about 1700 m/s. Within this cone it is difficult, if not impossible, to trace reflections with the receiver spacing used. Any reflections arriving at late times will be masked by this cone. When this groundwater-bearing
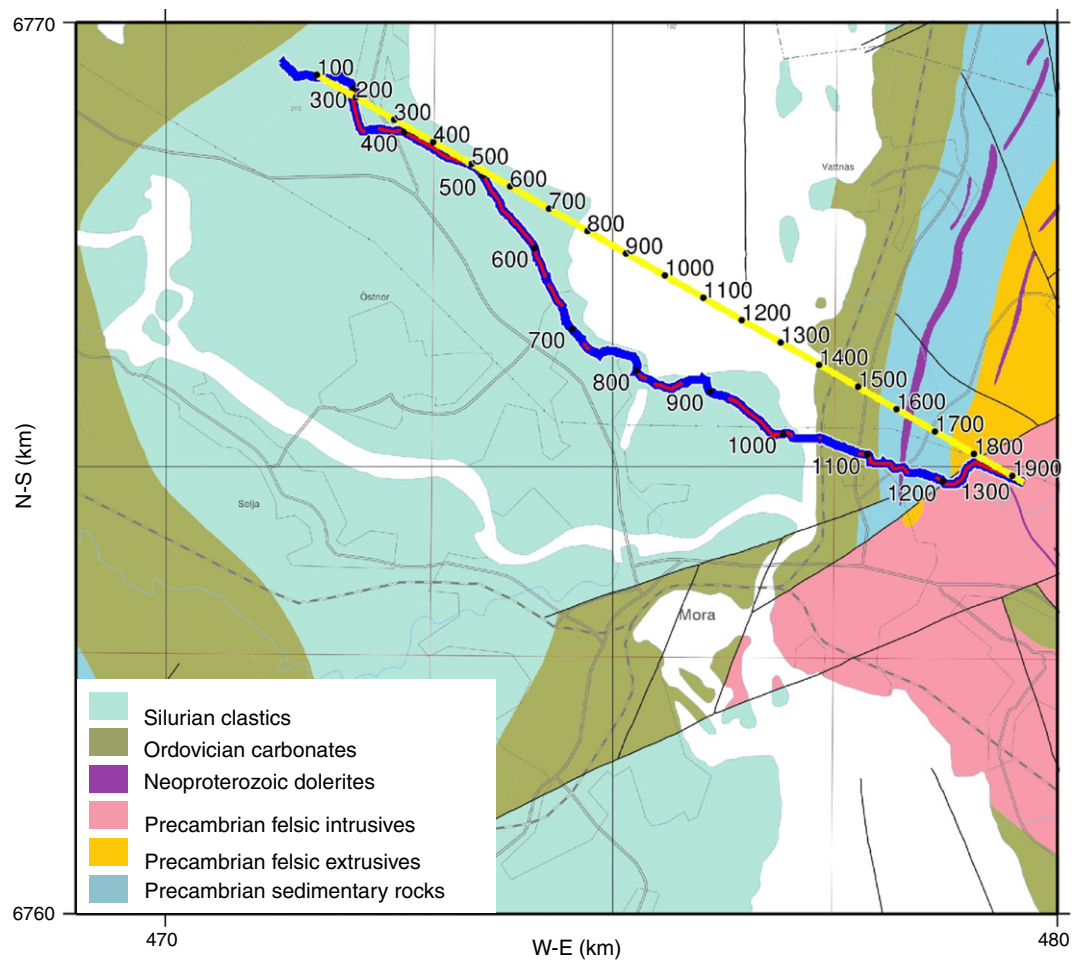
Fig. 3. Mora profile location. Blue line indicates where the geophones were placed. When filled with red then the source was activated at those locations along the profile. Yellow line shows the CDP processing line that the data were stacked along. Geological background map provided by the Geological Survey of Sweden (www.sgu.se).

layer of loose sediments is thinner or absent this cone is less prevalent (Fig. 5a, left side of spread) and reflections are more easily observed in raw source gathers. The thickness of this problematic layer varies considerably along the Mora profile, while along the Orsa profile this layer is less of a problem and appears to be present mainly in the southern part of the profile where fluvial sediments are present at the surface (Fig. 6a). Further north along the Orsa profile the data quality is generally good with clear first arrivals across the entire spread (Fig. 6b). Note how the apparent velocity increases at the further offsets in Figs. 5a and 6b, indicating higher velocity rock at depth.

The variable data quality along the profiles, especially the Mora profile, along with variable velocities, both vertically and horizontally, was a processing challenge. It is difficult to estimate the velocity in the dry loose deposits since the direct wave through them is only recorded on the closest geophone or two, but based on these arrivals a velocity of 600 m/s is reasonable for these deposits. When water saturated, these loose deposits have a velocity on the order of 1700 m/s. The first main refractor that is observed has a velocity of about 3000–3200 m/s, corresponding to the uppermost Paleozoic rocks. A deeper refractor is sometimes observed with a velocity on the order of 4000–4200 m/s that probably represents a deeper succession of Paleozoic rocks. East of the Lake Orsa outlet on the Mora profile, refractor velocities of about 5000 m/s are observed.

Both profiles followed roads and forest tracks, resulting in crooked line data being acquired. One option for handling such data is to define a slalom stacking line that follows the general trend of the mid-points. However, this strategy can result in false structures being introduced into the final stacks where the profile changes direction rapidly (e.g. Wu et

al., 1995). Instead, straight stacking lines were used with Common Data Point (CDP) bins defined perpendicular to the stacking line with the true acquisition geometry still being honored. That is, it was not assumed that the data had been acquired along straight lines. Since the stacking (or CDP) lines are straight they can be shifted at will in the direction normal to them and the same result will be obtained in the processing. Therefore, the location of the stacking lines in Figs. 3 and 4 is only schematic, and they may be shifted as explained above without affecting the processing results.

Mostly standard processing steps were applied to the data after CDP binning. Due to that most of the reflections are observed best at wide angles a large normal NMO stretch was allowed. This large stretch reduces the apparent frequency content of the data in the stacked sections. However, if the maximum stretch was decreased to a more normal value of 40% then some reflections were completely muted in the source gathers and no additional reflections appeared in the stacks. Increasing the allowable stretch to above 70% did not only increase amplitudes in the stacked sections, but also decreased the frequency content even more. A stretch value of 70% in the NMO processing step therefore seemed to be a reasonable compromise. Due to the often 'ringy' nature of the data in the Mora profile and the more prevalent noise cone, both a top mute and a bottom mute were applied before stacking. Top muting was to ensure that first arrivals were not stacked in as reflected energy. Bottom muting was applied to reduce the influence of the noise cone in the uppermost 300 ms of the stacked section. A complete list of processing steps for the two profiles is provided in Table 2.
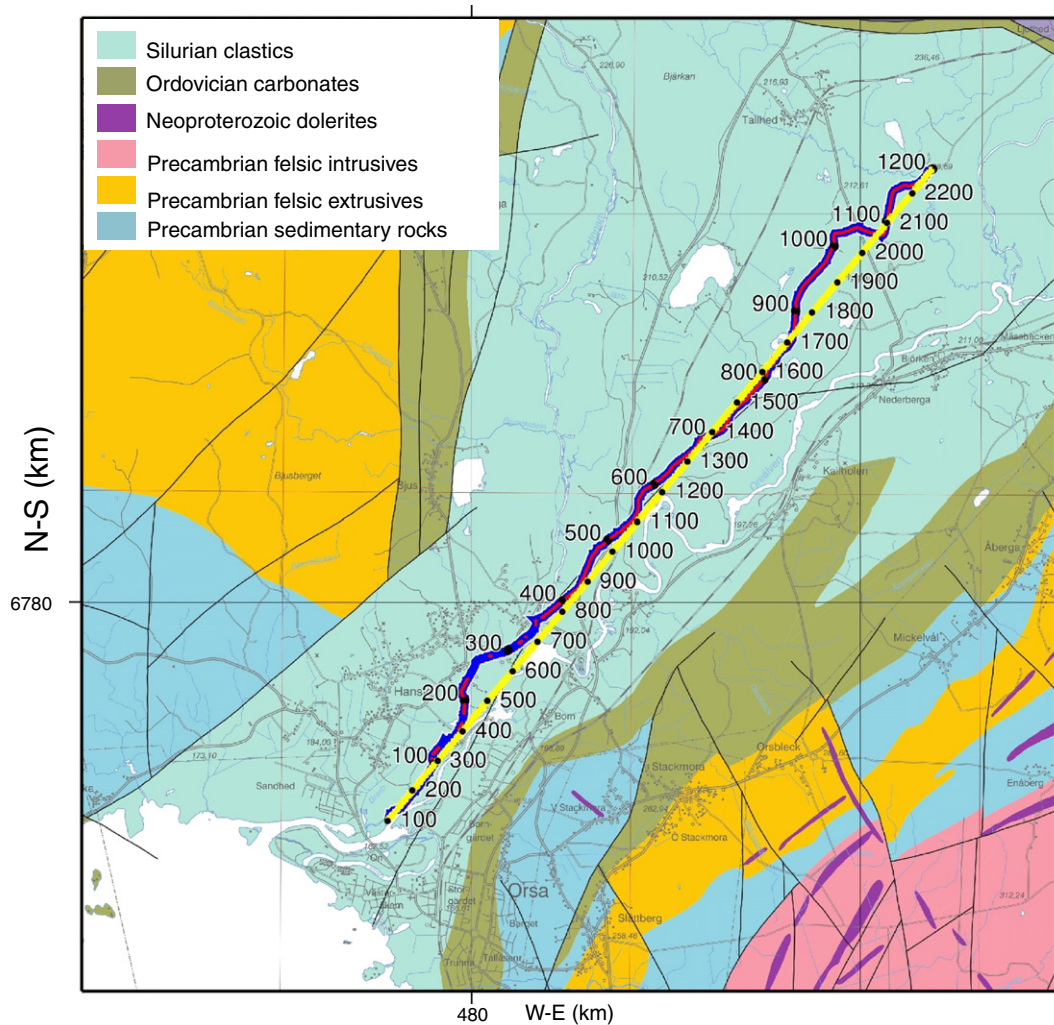
Fig. 4. Orsa profile location. Blue line indicates where the geophones were placed. When filled with red then the source was activated at those locations along the profile. Yellow line shows the CDP processing line that the data were stacked along. Geological background map provided by the Geological Survey of Sweden (www.sgu.se).

5. Results

Stacked and migrated sections are shown for the Mora and Orsa profiles in Figs. 7 and 8, respectively.

The Mora profile is characterized by reflective packages of variable dip with the only longer clear sub-horizontal reflection being present in the west between CDPs 350 and 700 at an approximate time of 200 ms (c. 250 m). The rest of the profile either shows a transparent seismic response, reflections with either a predominantly easterly or westerly dip, or shorter packages of sub-horizontal reflections (Fig. 7). There are no clear reflections from below 500 ms. Note the generally higher frequency content in the data east of CDP 1500 where the bedrock consists of Ordovician carbonate rocks and Precambrian crystalline rocks. Dipping events in the upper 400 ms, with opposite dips, between CDPs 500 and 700 may be from real steeply dipping structures since they have apparent velocities of about 3500 m/s. However, they may also result from direct or surface waves that have not been removed entirely during the processing. The more moderately, mainly east dipping events, between CDPs 800 and 1000 probably represent a sub-surface structure that has been significantly disturbed.

The Orsa profile shows a more consistent image with mainly sub-horizontal reflections present in the uppermost 400 ms throughout the profile (Fig. 8). Only in the south are transparent zones present, between CDPs 100 to 300 and 550 to 650. Dipping reflections are most apparent between CDPs 300 and 500 in the south and in the northernmost

part of the profile around CDP 2200. A deeper sub-horizontal reflective zone is present in the central parts of the profile between 800 and 900 ms. There are also indications of dipping reflections above this sub-horizontal reflectivity. Evidence for faulting is present throughout most of the section. Faults with minor throws are obvious between CDPs 1250 and 1700 in the upper 200 ms. Further north, between CDPs 1750 and 2000, a graben-like structure is present in the upper 400 ms containing faults with throws on the order of 100 ms (200 m).

6. Seismic modeling

Based on the refractions observed in the source gathers and the presence of wide-angle reflections there are clear velocity contrasts in the sub-surface along the profiles that can produce reflections. However, the stacked and migrated images show a complex and sometimes sporadic reflectivity pattern that is difficult to interpret based on geometry alone. It is not even clear if the crystalline Precambrian basement has been imaged along the profiles when only inspecting the stacked sections. To aid in the interpretation, CDP super gathers of the raw data were generated to allow velocity as a function of depth (time) to be estimated along the profiles (Fig. 9). Data from five adjacent CDPs were binned at an offset interval of 10 m and then stacked within common offset bins so that only one trace is presented for each offset in the super gathers. On most super gathers there are clear breaks in the slope of the first arrivals with the slope decreasing with offset, indicating the
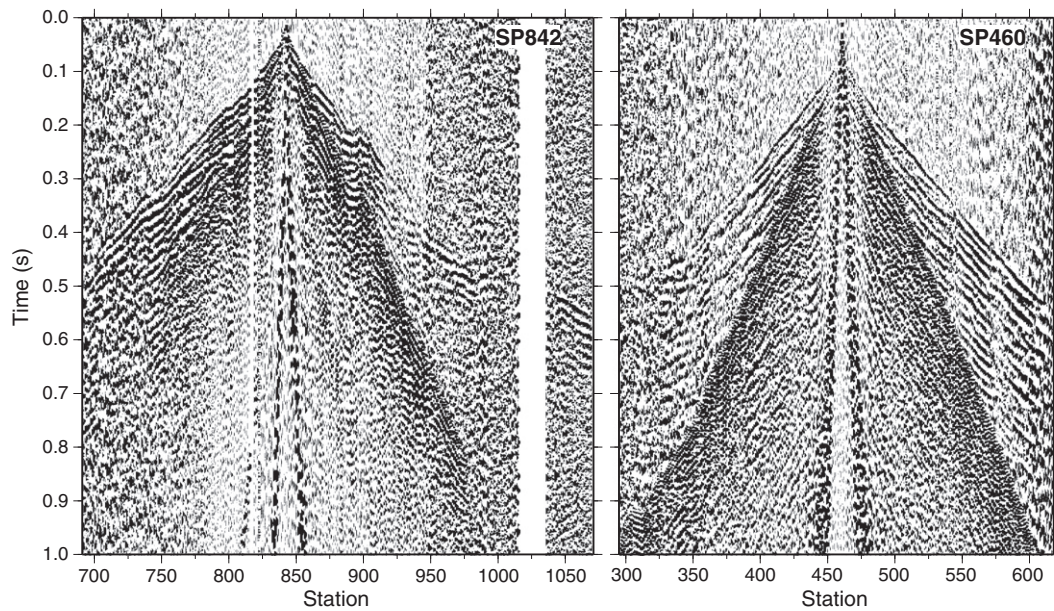
Fig. 5. (left panel) Source gather from SP 842 on the Mora profile (Fig. 3) showing a relatively small delay in the zero crossing of the main first break energy which indicates that the slow dry near-surface loose deposits are relatively thin at this source location. (right panel) Source gather from SP 460 on the Mora profile (Fig. 3) showing a longer delay in the zero crossing, a ringy signal after the first arrival and a cone multiple noise. The latter two characteristics of the data are probably due to a relatively thick groundwater layer at this location which energy gets trapped in.

arrival of refractions from deeper layers. The arrival times were then modeled for every 50th CDP assuming a horizontally layered sub-surface and increasing velocity with depth to generate velocity-depth models along the profiles. The assumption of a horizontally layered sub-surface is true along much of the profiles, but is obviously violated on some parts. Dipping layers and rapid lateral variations in velocity can significantly perturb the arrival times compared to the 1D assumption.

However, the velocity-depth models do show general consistency along the profiles and aid in the interpretation of the reflection seismic images.

As a further check on the modeling, synthetic seismograms were generated based on the obtained velocity-depth models using an elastic modeling program (Juhlin, 1995). Poisson's ratio was assumed to be on the order of 0.33 and the density increasing with increasing
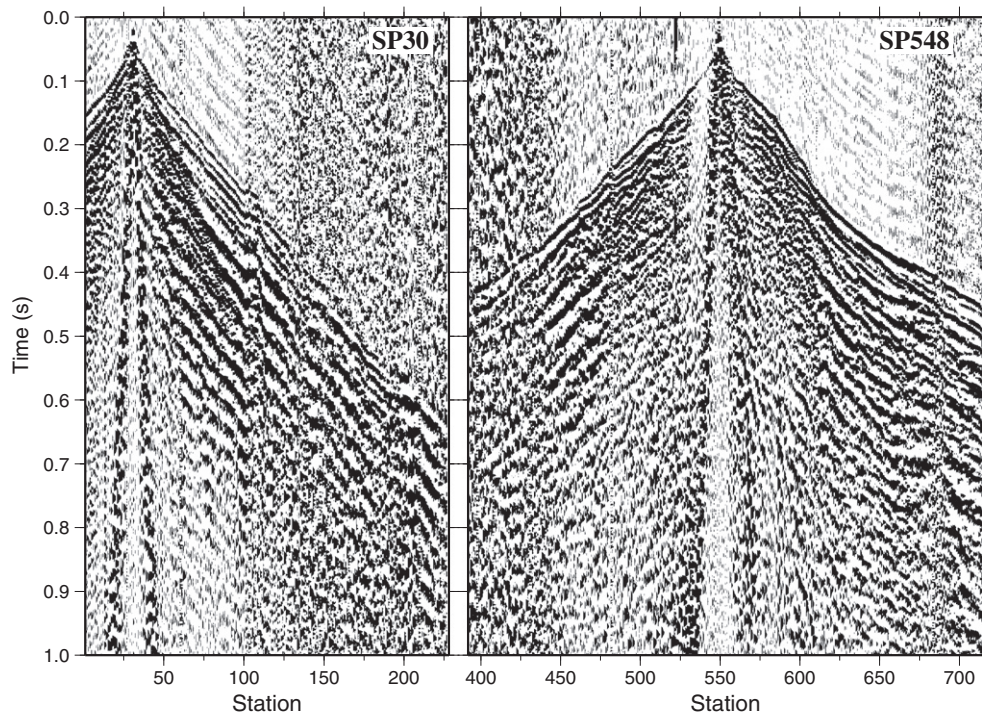

Fig. 6. (left panel) Source gather from SP 30 on the Orsa profile (Fig. 4) showing a moderate delay in the zero crossing of the main first break energy, a 'ringy' signal after the first arrivals and some signs of a noise cone due to trapped energy in the groundwater layer. (right panel) Source gather from SP 460 on the Orsa profile (Fig. 4) showing a typical response from the more northern part of the profile. Here, the ringyness is less prevalent and the multiple noise cone is generally absent.
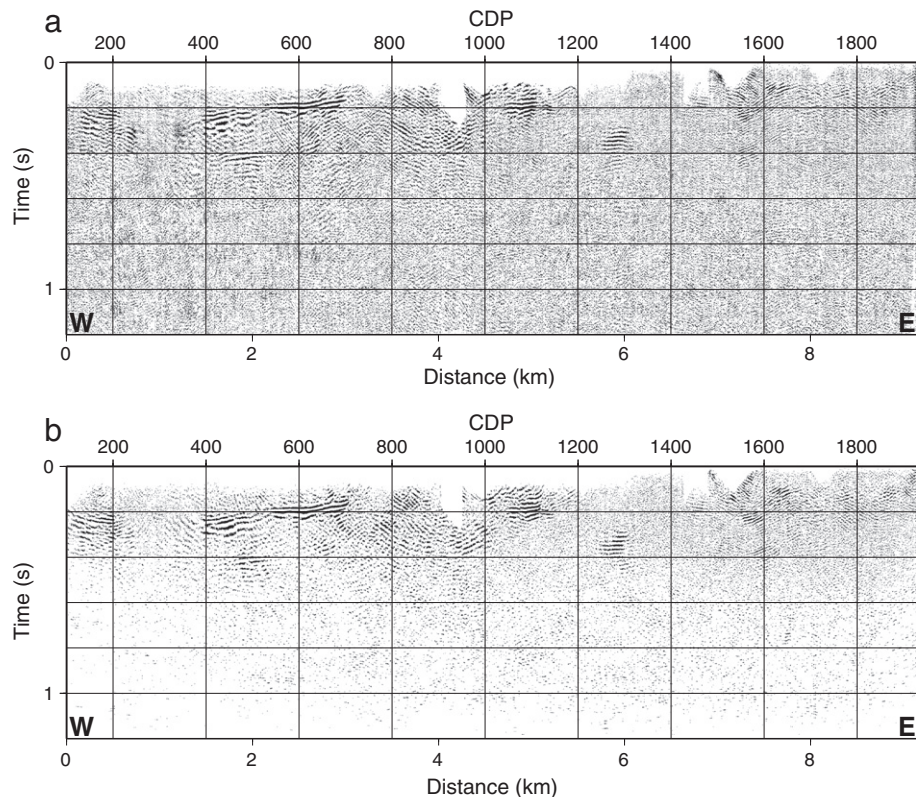
Table 2
Data processing.

Step	Parameters	
	Mora	Orsa
1	Read decoded VIBSIST data	
2	Bulk static shift to zero time	
3	Apply geometry	
4	Pick first breaks	
5	Spherical divergence correction	
6	Trace editing	
7	Trace balance: 0–3000 ms	
8	Spectral equalization:	
	0–600 ms: 50–80–200–240 Hz	
	700–1500 ms: 40–70–180–240 Hz	
9	Time variant bandpass filter:	
	0–400 ms: 50–80–240–360 Hz	
	450–600 ms: 45–70–210–300 Hz	
	700–1000 ms: 40–60–180–270 Hz	
	1100–3000 ms: 35–50–150–225 Hz	
10	Refraction statics: datum 160 m, replacement velocity 3000 m/s	Refraction statics: datum 180 m, replacement velocity 3000 m/s
11	Residual statics	
12	Median filter: 11 traces, 3 samples, 5300 m/s, subtract	Median filter: 11 traces, 3 samples, 1600, 2000, 2400 m/s, subtract
13	AGC: 50 ms	
14	Mute: top and bottom	No mute
15	Residual statics	
16	Velocity analysis	
17	NMO correction: 70% stretch mute	
18	Trace balance	
19	FX Decon: 19 trace window	
20	No dip filter	Dip filter 1.5 ms/trace cutoff
21	Trace balance	
22	Stolt migration: 200–3000, 1000–4000 ms/s	

P-wave velocity for the modeling. Fig. 9a shows a CDP super gather at CDP 600 on the Mora profile (Fig. 7), a location where the structure appears to be relatively sub-horizontal. The first arrivals calculated from the velocity-depth model (Table 3) match well with the observed first arrivals (Fig. 9a). Note that the low velocity unsaturated loose deposits (layer 1 in Table 3) appear to be relatively thick here (17 m), but that signals are still clear out to 1500 m offsets in the real data. Most of the general characteristics of the modeled data agree well with observations in the real data. In particular, the strong multiples, both reflected and refracted, and the noise cone due to the water saturated loose sediments (layer 2 in Table 3) are similar in the two sections (Fig. 9a). One discrepancy is the reflected wave from the base of layer 3 that arrives earlier in the modeled data than in the real data. The reason for this is not clear, but could be related to anisotropy, with propagation velocities faster in the horizontal direction than in the vertical direction. Further west, at CDP 300 (Fig. 9b), the first arrivals are less clear at far offsets in spite of low velocity layer 1 being thinner (Table 3), implying that other factors are affecting the data quality than the uppermost dry loose sediments. First arrivals are modeled well by a 5 layer model, but there is no clear reflection from the base of layer 4 (the equivalent to layer 3 at CDP 600). This may be due to the interface being disturbed at this location or generally poorer data quality in this area. Reflections at this location are also absent on the stacked section (Fig. 7). Note that the noise cone is not modeled as well here as at CDP 600. Further east, at CDP 1300 (Fig. 9c), first arrivals from the equivalent of layer 3 at CDP 600 and layer 4 at CDP 300 are absent. Instead first arrivals from a layer with a slope corresponding to 1550 m/s are present to offsets of almost 500 m. A refracted wave with an apparent velocity of 5100 m/s then arrives first out to about 800 m. At greater offsets it is more difficult to identify the first arrival, but the apparent velocity increases up to about 7500 m/s, a very high value. Significant multiple energy is also present in the synthetic data as is a noise cone that corresponds well in time with the real data. The reflection from the base of layer 2 arrives within this noise. Therefore, it is unlikely that this reflection would be imaged on the real data, although signs of it are present.

The velocity-depth models that were determined along both profiles have been plotted onto the stacked migrated sections to aid in

Fig. 7. Mora profile showing the (a) stacked and (b) migrated sections.
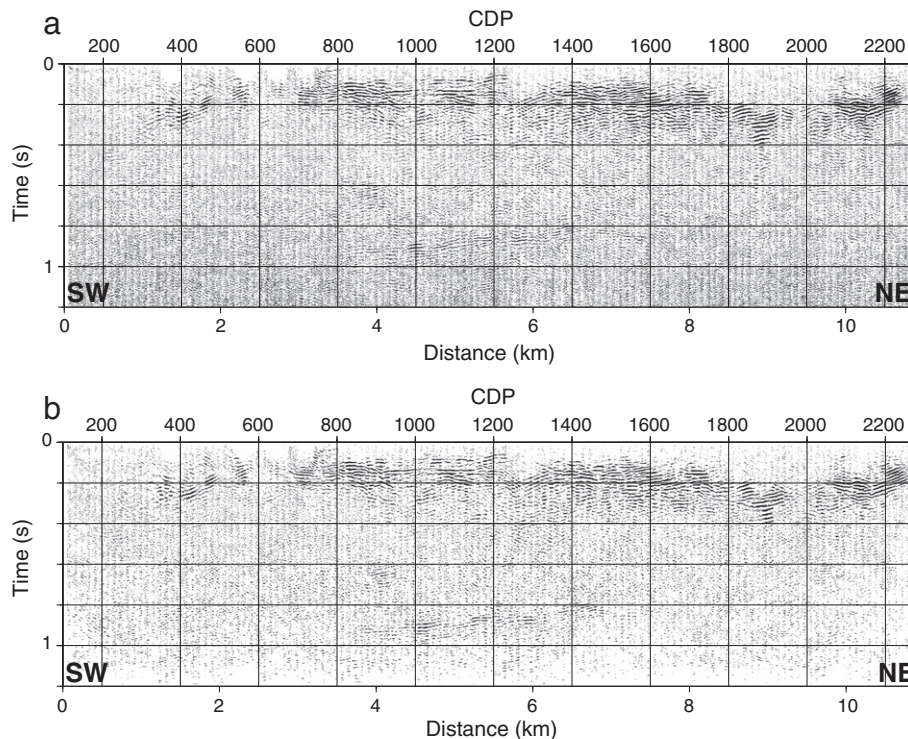
Fig. 8. Orsa profile showing the (a) stacked and (b) migrated sections.

the interpretation (Figs. 10 and 11). Prior to plotting, the depths were converted to time and a static shift corresponding to the refraction static correction at each CDP location was applied. This allows a rough comparison to be made between the refraction models and the reflection images. The refraction models and the interpretation of the reflections images are discussed in the next section.

7. Discussion

The reflection seismic images do not show a simple layered structure along the profiles, indicating that complex geological conditions are present in some parts. Interpretation of the profiles based solely on the reflection images is difficult. However, the modeled refractors aid significantly in the interpretation, especially if lithologies can be assigned to the velocities. Unfortunately, no velocity logs are available through the sedimentary successions from any of the boreholes. Therefore, we have assumed the following in our interpretation: velocities less than 2100 m/s correspond to glacial sediments, velocities in the range of 2500–3200 m/s correspond to Silurian clastic rocks, velocities in the range of 3800–4200 m/s correspond to Ordovician limestones, velocities in the range of 4500–5500 m/s correspond to highly fractured crystalline rock or Precambrian meta-sedimentary/volcanic rocks and velocities greater than 5500 m/s correspond to mainly intact crystalline bedrock.

In the Mora section (Fig. 10), the refractor velocity corresponding to the interpreted top of the Silurian is relatively consistent along the profile at about 3000–3200 m/s. This refractor is only present in the southern and northern parts of the Orsa profile (Fig. 11), indicating the Silurian to be thinner here, or perhaps absent in the central part. The interpreted refraction velocity at the top of the Ordovician is generally

higher and more variable in the Orsa profile than in the Mora profile. In addition, the velocities below the base of the interpreted Ordovician on the Orsa profile are high at about 6000 m/s, indicating intact crystalline basement is present. On the Mora profile, first arrivals with such a high apparent velocity are not observed, except at CDP 1300, suggesting that the crystalline basement is deeper and has not been mapped. At around CDP 1300 (Fig. 9c) higher apparent velocities are observed, but this is very local. The 5100 m/s velocities at CDP 1300 are probably too low to represent intact crystalline basement and the 7500 m/s velocity may be due to geometrical effects or to a high velocity mafic intrusion at depth. The deeper reflections corresponding to this high velocity boundary are also a sign of a strong impedance contrast at depth (Fig. 10).

The only clear reflection from within the basement is observed on the Orsa profile, a gently dipping event at about 900 ms (Fig. 11). Given that sub-horizontal reflections further east at similar depths are generated by thin dolerite sills (e.g. Juhlin, 1990), it is likely that this reflection also is generated from a dolerite sill at about 2 km depth. However, it is also possible that it represents a detachment surface on which mega-blocks have slid. Therefore, it is of interest to drill through the interface generating this reflection.

Recent studies of new drill cores in the Siljan Ring (Lehnert et al., 2012) have shown that the classical distribution in the Siljan area of an Ordovician carbonate platform followed by Silurian shales and mudstone and the Silurian/Devonian terrestrial Orsa Sandstone has to be re-evaluated and ancient facies belts have to be reconstructed in detail for different time slices. The development of the Lower–Middle Ordovician carbonate succession, from the contact to the Precambrian basement to the upper part of an overlying limestone (Holen Formation) is approximately uniform across the Siljan district at about 20 m. In the Mora area this limestone exhibits exposure plus erosion, interpreted as

Fig. 9. CDP super gathers with corresponding elastic modeling at CDP locations (a) 600, (b) 300 and (c) CDP 1300 along the Mora profile. Blue lines represent the first break times calculated from the velocity-depth models in Table 3 while the green line represents the reflection time corresponding to the base of layer 3 for CDP 600, the base of layer 4 for CDP 300 and the base of layer 2 for CDP 1300. Data area plotted with at reduced times with the reduction velocity given by RVEL.
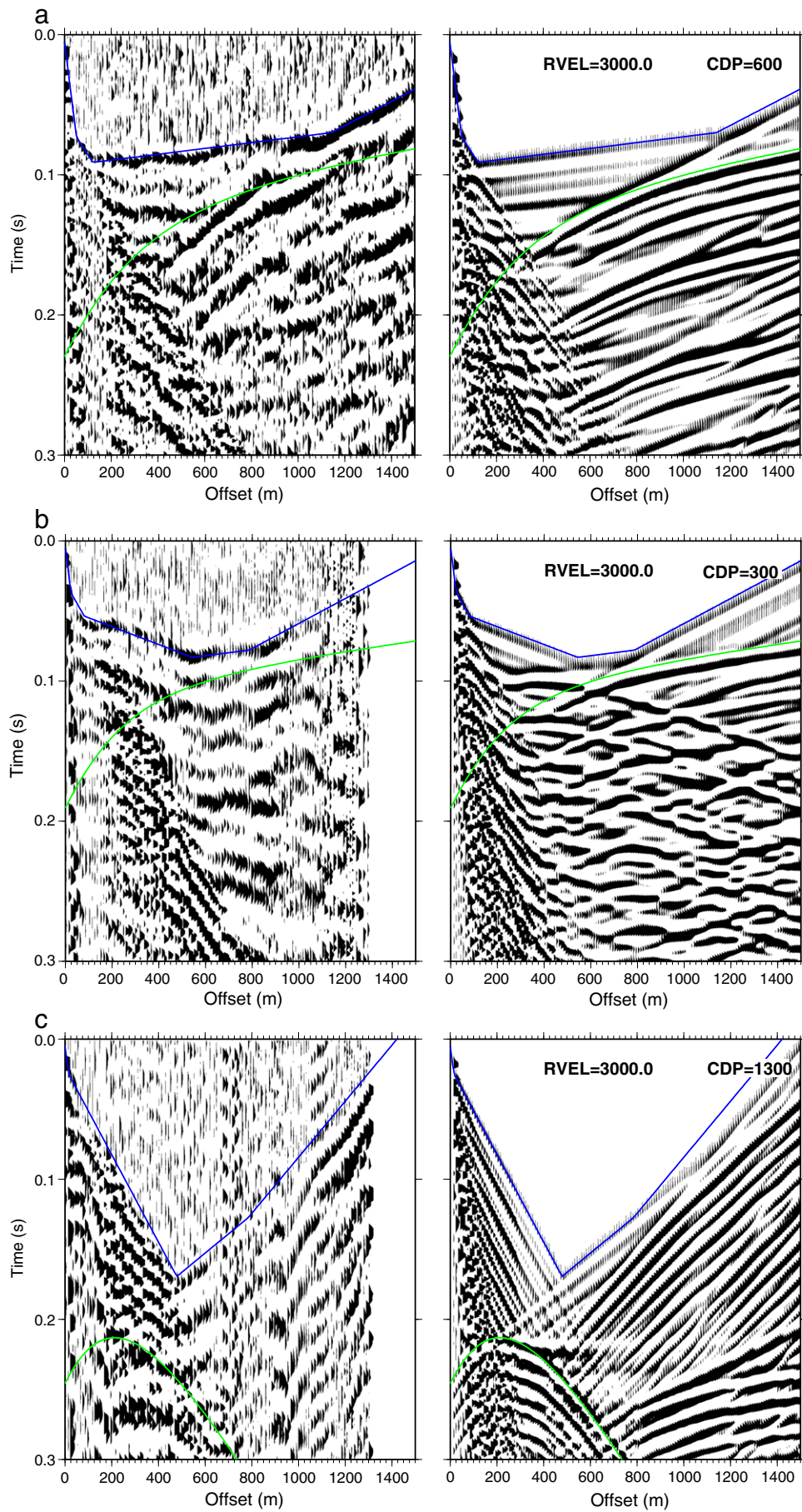
Table 3
Modeling parameters used for Fig. 9. HS refers to a half-space.

Layer	CDP 300		CDP 600		CDP 1300	
	Base depth (m)	Vp (m/s)	Base depth (m)	Vp (m/s)	Base depth (m)	Vp (m/s)
1	8	600	17	600	5	600
2	27	1600	50	1700	179	1550
3	120	2520	254	3200	402	5100
4	217	3200	HS	4050	HS	7500
5	HS	4100				

Fig. 10. Interpreted Mora profile. Times to refractors are plotted as short red lines at those CDP locations where a reasonable time-offset curve for the first arrivals could be picked. The velocity of the refracting interface is shown below each red line. Shown also are interpretations of the boundaries of the different geological units based on the reflection seismic images and the refraction interpretation. Yellow—base of the water saturated loose sediments, green—base of the Silurian, blue—base of the Ordovician, black—dolerite intrusion, gray—fault.

due to the formation of a peripheral bulge in the Caledonian foreland basin. Later, the limestone was covered by a more than 200 m thick Silurian clastic succession. This Silurian shale basin in the Mora area (probably thinning or partially eroded towards the east) may partly explain why the basement is apparently deeper along the Mora seismic profile than along the Orsa profile.

The only location along the Mora profile that the reflection seismic data indicate a relatively undisturbed layering of the sedimentary successions is between CDPs 350 and 700. Here the interpreted top of the Ordovician corresponds to a clear seismic reflection, indicating little internal deformation, and the refraction modeling indicates the Silurian to be about 200 m thick below CDP 600 (Table 3). If the deeper reflection at 0.4 s (Fig. 10) corresponds to the top of the basement then the unit below is about 400 m thick, giving a total thickness of the Paleozoic successions of about 600 m here. Whether the lowermost unit consists entirely of Ordovician limestones or whether there may be Cambrian units present at depth cannot be determined from the seismic data. On the rest of the Mora profile there are only short segments where reflections directly correlate with the results from the refraction interpretation, indicating that the sedimentary successions are heavily disturbed. The depth to the crystalline basement is relatively well determined along the Orsa profile, generally being on the order of 200–300 m, except south of CDP 500 and in the heavily faulted northern part of the profile (CDPs 1750 to 2000) that was mentioned earlier. This is significantly less than along the Mora profile, suggesting that the facies may be different north of Lake Orsa compared to that found in the Mora area.

Intense thrusting during the emplacement of megablocks is observed in the yet to be described Stumsnäs 1 (Fig. 1) core of Igrene AB (repeated thrusting of granitic basement over fault-bounded Ordovician limestone units) and the Nittsjö trench (Fig. 1) (thrust slices of Lower/Middle Ordovician marls in structural contact with Proterozoic meta-volcanoclastics). In addition, the occurrence of a Silurian clastic succession (Nederberga

Formation), a facies typical of the Silurian shale basin in the western part of the impact structure, in the north-central part of the ring structure at Skattungbyn reflects also some large-scale overthrusting and not simple sliding of blocks from the rim of the crater towards the central uplift. Similar thrusting may be expected to be present in the Mora area and may explain the lack of coherency of reflections along most of the Mora profile.

8. Conclusions

The reflection seismic data presented here shed new light on the Paleozoic successions in the western Siljan Ring. They show a complex and disturbed reflection pattern, especially along the Mora profile. Reflections are more coherent on the northern Orsa profile. Interpretation of the reflection images was greatly aided by combining information from refraction modeling, allowing depths to the top of Ordovician limestone to be estimated along both profiles.

New core data from a borehole drilled in the town of Mora shows a thick Silurian shale sequence (more than 200 m) above the Ordovician limestone in this part of the Siljan Ring. Where reflections are clear from the interpreted base of the Silurian on the Mora seismic profile (CDPs 350 to 700) we estimate the Silurian to be about 200 m thick, indicating that this shale sequence extends at least this far to the north. Depth to the crystalline bedrock is generally greater along the Mora profile than the Orsa profile, with the Paleozoic successions interpreted to be as thick as 600 m in the western part of the Mora profile. Both the reflection images and the refraction interpretation indicate the bedrock to be highly faulted. In the northern part of the Orsa profile the data indicate normal faults with throws of up to 200 m. Significant faulting of the bedrock is also interpreted in the eastern part of the sedimentary successions on the Mora profile.

In order to study the distribution of significant sedimentary changes (limestones vs. shales vs. sandstone units) and to reconstruct the
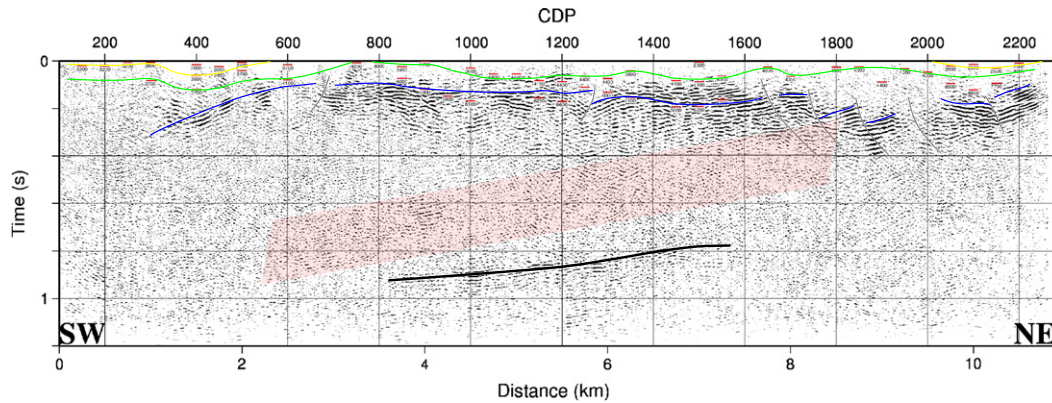
Fig. 11. Interpreted Orsa profile. Times to refractors are plotted as short red lines at those CDP locations where a reasonable time-offset curve for the first arrivals could be picked. The velocity of the refracting interface is shown below each red line. Shown also are interpretations of the boundaries of the different geological units based on the reflection seismic images and the refraction interpretation. Yellow—base of the water saturated loose sediments, green—base of the Silurian, blue—base of the Ordovician, black—dolerite intrusion, gray—fault, pink area—possible reflective zone in the Precambrian basement.

extension of coeval facies belts, the position of megablocks and thrust slices, higher resolution shallow seismic studies together with new drill cores are required. One new core must include the Silurian siliciclastic succession in the Orsa area, where lithostratigraphic control is needed for seismic interpretation of the data reported here. Future higher resolution shallow seismic studies will help to document the contacts between various Silurian sandstone and shale units as well as between Silurian siliciclastics and underlying Ordovician shelf carbonates resting on Precambrian basement rocks. Both additional seismic data and shallow drilling are required before the location of a deeper borehole can be finalized.

References

Bergström, S.M., 2007. The Ordovician conodont biostratigraphy in the Siljan region, south-central Sweden: a brief review of an international reference standard. In: Ebbestad, J.O.R., Wickström, L.M., Högström, A.E.S. (Eds.), WOGOGOB 2007. 9th Meeting of the Working Group on Ordovician Geology of Baltoscandia. Field Guide and Abstracts: Sveriges Geologiska Undersökning Rapporter och Meddelanden, 128, pp. 26–41. 63–78.

Bodén, A., Erikson, K.G., 1988. Deep Drilling in Crystalline Bedrock; Vol. 1: The Deep Gas Drilling in the Siljan Impact Structure, Sweden and Astroblemes. Springer Verlag, Berlin . 364 pp.

Collini, B., 1988. Geological Setting of the Siljan Ring Structure Deep Drilling in Crystalline Bedrock, Vol. 1: The Deep Gas Drilling in the Siljan Impact Structure, Sweden and Astroblemes. Springer Verlag, Berlin, pp. 349–354.

Ebbestad, J.O.R., Högström, A.E.S., 2007. Ordovician of the Siljan district, Sweden. In: Ebbestad, J.O.R., Wickström, L.M., Högström, A.E.S. (Eds.), WOGOGOB 2007. 9th meeting of the Working Group on Ordovician Geology of Baltoscandia. Field guide and Abstracts: SGU Rapporter och meddelanden, 128, pp. 7–26.

Grieve, R.A.F., 1988. The formation of large impact structures and constraints on the nature of Siljan. In: Boden, A., Eriksson, K.G. (Eds.), Deep Drilling in Crystalline Bedrock. : The Deep Gas Drilling in the Siljan Impact Structure, Sweden and Astroblemes, Proceedings of the International Symposium, vol. 1. Springer Verlag, Berlin, pp. 328–348.

Henkel, H., Aaro, S., 2005. Geophysical investigations of the Siljan impact structure—a short review. In: Koeberl, Henkel, H. (Eds.), Impact Tectonics. Springer Verlag, Berlin, pp. 247–283.

Högström, A.E.S., Sturkell, E., Ebbestad, J.O.R., Lindström, M., Ormö, J., 2010. Concentric impact structures in the Palaeozoic of Sweden—the Lockne and Siljan craters. GFF 132, 65–70.

Holm, S., Alwmark, C., Alvarez, W., Schmitz, B., 2011. Shock barometry of the Siljan impact structure, Sweden. Meteoritics and Planetary Science 46, 1888–1909.

Juhlin, C., 1990. Interpretation of the reflections in the Siljan Ring area based on results from the Gravberg-I borehole. Tectonophysics 173, 345–360.

Juhlin, C., 1995. Finite difference elastic wave propagation in 2-D heterogeneous transversely isotropic media. Geophysical Prospecting 43, 843–858.

Juhlin, C., Pedersen, L.B., 1987. Reflection seismic investigations of the Siljan impact structure, Sweden. Journal of Geophysical Research 92, 14113–14122.

Juhlin, C., Pedersen, L.B., 1993. Further constraints on the formation of the Siljan impact crater from seismic reflection studies. Geologiska Föreningens i Stockholm Förhandlingar 115, 151–158.

Juhlin, C., Dehghannejad, M., Lund, B., Malehmir, A., Pratt, G., 2010. Reflection seismic imaging of the end-glacial Pärvie Fault system, northern Sweden. Journal of Applied Geophysics 70, 307–316.

Juhojuntti, N., Juhlin, C., 1998. Seismic lower crustal reflectivity and signal penetration in the Siljan Ring area, Central Sweden. Tectonophysics 288, 17–30.

Kenkmann, T., von Dalwigk, I., 2000a. Centro-symmetrical material flow during crater modification: structural implications. Lunar and Planetary Science Conference XXXI, Abstract 1041.

Kenkmann, T., von Dalwigk, I., 2000b. Radial transpression ridges: a new structural feature of complex impact craters. Meteoritics and Planetary Science 35, 1189–1202.

Lehnert, O., Meinhold, G., Bergström, S.M., Calner, M., Ebbestad, J.O.R., Egenhoff, S., 597 Frisk, Å.M., Hannah, J.L., Högström, A.E.S., Huff, W.D., Juhlin, C., Maletz, J., Stein, H.J., Sturkell, E., Vandenbroucke, T.R.A., 2012. New Ordovician-Silurian drill cores from the Siljan impact structure in central Sweden - an integral part of the Swedish Deep Drilling Program. GFF 134, 87–98. http://dx.doi.org/10.1080/11035897.2012.692707.

Lorenz, H., 2010. The Swedish Deep Drilling Program: for science and society. GFF 132, 25–27.

Papasikas, N., Juhlin, C., 1997. Interpretation of reflections from the central part of the Siljan Ring impact structure based on results from the Stenberg-1 borehole. Tectonophysics 269, 237–245.

Park, C.B., Miller, R.D., Steeples, D.W., Black, R.A., 1996. Swept impact seismic technique (SIST). Geophysics 61, 1789–1803.

Petalas, C., 1985. Sedimentary petrology of the Orsa sandstone, central Sweden. UUDMP research report, 40, pp. 1–138.

Reimold, W.U., Kelley, S.P., Sherlock, S., Henkel, H., Koeberl, C., 2004. Laser argon dating of melt breccias from the Siljan impact structure, Sweden—implications for possible relations to late Devonian Extinction events. Lunar and Planetary Science Conference, XXXV, Abstract 1480.

Reimold, U., Kelley, S.P., Sherlock, S., Henkel, H., Koeberl, C., 2005. Laser argon dating of melt breccias from the Siljan impact structure, Sweden: implications for a possible relationship to Late Devonian extinction events. Meteoritics and Planetary Science 40, 591–607.

Rondot, J., 1975. Comparison entre les astroblemes de Siljan, Suede et de Charlevoix, Quebec, vol. 6. Bulletin of the Geological Institute of the University of Uppsala, N.S., pp. 85–92.

Wu, J., Milkereit, B., Boerner, D.E., 1995. Seismic imaging of the enigmatic Sudbury Structure. Journal of Geophysical Research 100 (B3), 4117–4130.